New BEDT-TTF Salts Incorporating the Hydrogen Dichloride (HCl_2^-) Anion

Brian H. Ward,† Garrett E. Granroth,§ Khalil A. Abboud,†
Mark W. Meisel,*,§ and Daniel R. Talham*,†

Department of Chemistry, University of Florida, Gainesville, Florida 32611-7200, and Department of Physics and Center for Ultralow Temperature Research, University of Florida, Gainesville, Florida 32611-8440

Received October 16, 1997. Revised Manuscript Received January 26, 1998

Salts of the π-donor bis(ethylenedithio)tetrathiafulvalene (BEDT-TTF) have been isolated with hydrogen dichloride (HCl_2^-) as the counterion. Two phases were obtained, α'-BEDT-$TTF_2(HCl_2)$ **(1)** and ϵ-BEDT-TTF(HCl_2) **(2)**, by electrocrystallization from solvent mixtures containing $ClCH_2COCl$. Like previously described α'-BEDT-TTF_2X salts, **1** contains sheets of twisted BEDT-TTF dimers, and conductivity and magnetic susceptibility are consistent with a description of nearly localized $(BEDT\text{-}TTF)_2^+$ radicals. Salt **2**, space group $C2/m$, undergoes an anion ordering structural phase transition near 200 K, resulting in a new low-temperature phase ϵ'-BEDT-TTF(HCl_2) **(3)** with space group $P2_1/c$. Below 170 K, **3** undergoes a magnetic phase transition seen in electron paramagnetic resonance data. The HCl_2^- ion is linear in **1** but bent in **2** and **3**. α'-$(BEDT\text{-}TTF)_2(HCl_2)$, **1**, crystallizes in the $P2/c$ space group with $a = 7.7023(1)$ Å, $b = 6.6140(1)$ Å, $c = 30.1077(6)$ Å, $\beta = 96.506(1)°$, $V = 1523.90(4)$ Å^3, and $Z = 2$. ϵ-BEDT-TTF(HCl_2), **2**, crystallizes in the $C2/m$ space group with $a = 12.9687(8)$ Å, $b = 11.6077(8)$ Å, $c = 5.6949(4)$ Å, $\beta = 104.688(1)°$, $V = 829.28(10)$ Å^3, and $Z = 2$. ϵ'-BEDT-TTF(HCl_2), **3**, belongs to the $P2_1/c$space group with $a = 12.7112(1)$ Å, $b = 11.5778(2)$ Å, $c = 11.3583(1)$ Å, $\beta = 101.194(1)°$, $V = 1639.77(3)$ Å^3, and $Z = 4$.

I. Introduction

The organic π-donor bis(ethylenedithio)tetrathiafulvalene (BEDT-TTF) is the basis of a large number of conducting and superconducting cation-radical molecular solids.[1−7] Conductivity in these materials occurs via the donor-ion network[3,8] made up of stacks or sheets of closely packed donor molecules. The most common route to pure crystalline samples of conducting cation-radical salts is through electrochemical oxidation of the donor in the presence of an appropriate counterion. Salts are generally formed where the oxidation state of the donor ranges from $+^1/_2$ to $+1$, and all of the current superconducting examples have donor oxidation states between 0 and 1.[4,9] Recently, the first dication salts of BEDT-TTF have been isolated as the tetrafluoroborate and perchlorate salts.[10,11] In these solids the donor BEDT-TTF exists only as the dication. The salts were prepared by electrocrystallization from an oxidizing solvent mixture, such that BEDT-TTF is first chemically oxidized to the monocation in solution followed by electrochemical oxidation to the dication.

Attempts to prepare further examples of high-oxidation state cation-radical salts have now resulted in the isolation of the first hydrogen dichloride (HCl_2^-) salts of BEDT-TTF. Two morphologies α'-BEDT-$TTF_2(HCl_2)$ **(1)** and ϵ-BEDT-TTF(HCl_2) **(2)** form simultaneously in the electrochemical cell. The physical properties of the 2:1 salt are quite similar to those of the existing α' salts,[12−14] and it incorporates the shortest linear anion in the series. The 1:1 (BEDT-TTF)HCl_2 material conforms to the ϵ-morphology[15] above 200 K and undergoes a structural transition below this temperature resulting

* Address correspondence to these authors.
† Department of Chemistry.
§ Department of Physics and Center for Ultralow Temperature Research.

(1) Williams, J. M.; Wang, H. H.; Emge, T. J.; Geiser, U.; Beno, M. A.; Leung, P. C. W.; Carlson, K. D.; Thorn, R. J.; Schultz, A. J.; Whangbo, M. *Prog. Inorg. Chem.* **1987**, *35*, 51−218.
(2) *Organic Superconductivity*; Kresin, V. Z., Little, W. A., Ed.; Plenum Press: New York, 1990; p 386.
(3) Cowan, D. O.; Wiygul, F. M. *Chem. Eng. News* **1986**, 28−45.
(4) Adrian, F. J.; Cowan, D. O. *Chem. Eng. News* **1992**, 24−41.
(5) *The Physics and Chemistry of Organic Superconductors*; Springer: Berlin, 1990; Vol. 51.
(6) Williams, J. M.; Kini, A. M.; Wang, H. H.; Carlson, K. D.; Geiser, U.; Montgomery, L. K.; Pyrka, G. J.; Watkins, D. M.; Kommers, J. M.; Boryschuk, S. J.; Strieby Crouch, A. V.; Kwok, W. K.; Schirber, J. E.; Overmyer, D. L.; Jung, D.; Whangbo, M. H. *Inorg. Chem.* **1990**, *29*, 3272−3274.
(7) Wang, H. H.; Geiser, U.; Williams, J. M.; Carlson, K. D.; Kini, A. M.; Mason, J. M.; Perry, J. T.; Charlier, H. A.; Crouch, A. V. S.; Heindl, J. E.; Lathrop, M. W.; Love, B. J.; Watkins, D. M.; Yaconi, G. A. *Chem. Mater.* **1992**, *4*, 247−249.
(8) Ferraro, J. R.; Williams, J. M. *Introduction to Synthetic Electrical Conductors*; Academia: San Diego, CA, 1987.
(9) Williams, J. M.; Ferraro, J. R.; Thorn, R. J.; Carlson, K. D.; Geiser, U.; Wang, H. H.; Kini, A. M.; Whangbo, M.-H. *Organic Superconductors*; Prentice Hall: Englewood Cliffs, NJ, 1992; p 400.
(10) Abboud, K. A.; Clevenger, M. B.; de Oliveira, G. F.; Talham, D. R. *J. Chem. Soc., Chem. Commun.* **1993**, 1560−1562.
(11) Chou, L. K.; Quijada, M. A.; Clevenger, M. B.; de Oliveira, G. F.; Abboud, K. A.; Tanner, D. B.; Talham, D. R. *Chem. Mater.* **1995**, *7*, 530−534.
(12) Beno, M. A.; Firestone, M. A.; Leung, P. C. W.; Sowa, L. M.; Wang, H. H.; Williams, J. M.; Whangbo, M. *Solid State Commun.* **1986**, *57*, 735−739.
(13) Ugawa, A.; Yakushi, K.; Kuroda, H.; Kawamoto, A.; Tanaka, J. *Synth. Met.* **1988**, *22*, 305−315.
(14) Obertelli, S. D.; Friend, R. H.; Talham, D. R.; Kurmoo, M.; Day, P. *J. Phys.: Condens. Matter 1* **1989**, 5671−5680.
(15) Abboud, K. A.; Chou, L. K.; Clevenger, M. B.; de Oliveira, G. F.; Talham, D. R. *Acta Crystallogr.* **1995**, *C51*, 2356−2362.

S0897-4756(97)00686-8 CCC: $15.00
Published on Web 03/18/1998

in a new phase ϵ'-BEDT-TTF(HCl_2) **(3)** below 185 K. The crystal structures and physical properties of the new hydrogen dichloride salts of BEDT-TTF are described.

II. Experimental Section

Materials Synthesis. BEDT-TTF was synthesized by the method of Larsen and Lenior.[16] Sodium phosphate (Na_3PO_4) and sodium chloride (NaCl) were obtained from Aldrich Chemical Co. (Milwaukee, WI) and used without further purification. Benzonitrile (C_6H_5CN, 99%), chloroacetyl chloride ($ClCH_2COCl$, 98%), and 1,4,7,10,13-pentaoxacyclopentadecane or 15-crown-5 ($C_{10}H_{20}O_5$, 98%) were purchased from Aldrich Chemical Co. (Milwaukee, WI). Benzonitrile was purified by distillation, and chloroacetyl chloride and 15-crown-5 were used without further purification. Methylene chloride (CH_2Cl_2, 99.9%) was purchased from Fisher Scientific (Orlando, FL), dried over P_2O_5, and distilled before use.

α'-(BEDT-TTF)$_2HCl_2$ (1) and ϵ-BEDT-TTF(HCl_2) (2). *Method 1.* BEDT-TTF (7.5 mg) was placed in the working arm of a two-electrode H-cell and dissolved in 30 mL of 9.75 mM sodium phosphate in 10% $ClCH_2COCl$/benzonitrile containing 10 drops of 15-crown-5. A constant current density of 0.90 $\mu A/cm^2$ was maintained at room temperature between the platinum working electrode and counter electrode that were separated by two glass frits. After a few days crystals could be seen on the electrode surface and at the bottom of the H-cell. No phosphate-containing salts were obtained, but small brown plates of **1** and large black needles of **2** were collected after 21 days, with the majority of the material forming as salt **1**.

Method 2. BEDT-TTF (7.5 mg) was placed in the working arm of a two-electrode H-cell and dissolved in 30 mL of 11.4 mM sodium chloride in 10% $ClCH_2COCl$/methylene chloride containing 10 drops of 15-crown-5 and oxidized as described above. The cells were maintained at room temperature with a constant current density of 0.90 $\mu A/cm^2$, and as above, both crystal forms were observed within a few days and were collected after 11 days.

Crystallographic Data Collection and Structure Determination. Data were collected at 173 K for **1** and **3** and at 233 K for **2** on a Siemens SMART PLATFORM equipped with a CCD area detector and a graphite monochromator utilizing Mo Kα radiation ($\lambda = 0.71073$ Å). Cell parameters were refined using 4947, 2211, and 6521 reflections for **1**, **2**, and **3**, respectively. A hemisphere of data for each structure (1381 frames) was collected using the ω-scan method (0.3° frame width). The first 50 frames were remeasured at the end of data collection to monitor instrument and crystal stability (maximum correction on I was <1%). Absorption corrections were applied based on the ψ-scan using the entire data sets.

All structures were solved by Direct Methods in SHELXTL5[17] and refined using full-matrix least-squares on F^2. In compound **1**, the asymmetric unit consists of one BEDT-TTF cation and one-half of an HCl_2^- anion. The non-H atoms were refined with anisotropic thermal parameters, whereas the H atoms were refined with isotropic thermal parameters except those associated with C14 and C16. One of the $-CH_2CH_2-$ (C14−C16) units in **1** is disordered and was refined in two partial units. Their site occupation factors refined to 0.76(1) and 0.24(1) and their H atoms were refined riding on the C atoms to which they are bonded. In compound **2**, the asymmetric unit consists of one-quarter of a BEDT-TTF cation and one-quarter of an HCl_2 anion, each located at a 2/m symmetry site. The CH_2 units are disordered and their occupation factors were fixed at 50% because of symmetry. The Cl atoms were also disordered and their occupation factors were fixed at 50% because of symmetry. In compound **3**, the asymmetric unit consists of one BEDT-TTF and one HCl_2 ion. The non-H atoms in **2** and **3** were treated anisotropically, whereas the hydrogen atoms were calculated in ideal positions and were riding on their respective carbon atoms.

Electron Paramagnetic Resonance (EPR) Measurements. An aligned mosaic of crystals of **1** and a single-crystal sample of **2** were mounted on a cut edge of a quartz rod, and EPR spectra were recorded on a Bruker (Billerica, MA) ER-200D spectrometer modified with a digital signal channel and a digital field controller. The system is equipped with an Oxford Instruments (Witney, England) ITC 503 temperature controller and ESR 900 cryostat supplied with an AuFe/Ch thermocouple. The temperature-dependent electron paramagnetic resonance data were obtained at 9.27 GHz with 100 kHz field modulation. Data were collected using a U.S. EPR (Clarksville, MD) SPEX300 data acquisition program.

SQUID Magnetometry Measurements. Susceptibility measurements were performed using a Quantum Design MPMS SQUID magnetometer operating at 1 kG on 31.25 mg sample of salt **1** that was physically separated from a mixture of salts **1** and **2**. A Teflon tube and plastic straw were used as the sample holder during the measurements. The background signals arising from the Teflon tube and straw were measured independently and subtracted from the raw data. Due to the atmospheric instability of salts **2** and **3**, magnetic susceptibility measurements were not performed.

Transport Measurements. Room temperature conductivity was measured by a four-probe method using narrow gauge (0.0127 mm diameter) gold wires affixed in a linear arrangement to a single platelike crystal ($0.59 \times 0.45 \times 0.05$ mm^3) of **1** using fast-drying gold paint.

III. Results and Discussion

The BEDT-TTF hydrogen dichloride salts were isolated during attempts to synthesize high-oxidation state salts of BEDT-TTF with high-valent counterions. The currently known high-oxidation state salts of BEDT-TTF, where BEDT-TTF exists only as the dication, include the tetrafluoroborate and perchlorate salts.[11] Since the counterions are monovalent, a high density is needed to compensate charge. The high concentration of anions around each donor molecule gives poor contact along and between stacks of donors. Incorporation of high-valent anions into the crystal lattice should provide charge compensation for the high oxidation state of the donor cations without a large concentration of anion species in the lattice.

The hydrogen dichloride BEDT-TTF salts were first obtained from a standard constant-current electrocrystallization cell using a 10% $ClCH_2COCl$/benzonitrile solvent mixture with Na_3PO_4 as the supporting electrolyte. Salts **1** and **2** were subsequently prepared using a 10% $ClCH_2COCl$/methylene chloride solvent mixture with NaCl as the supporting electrolyte. The hydrogen dichloride anion is believed to form after reduction and homolytic bond cleavage of $ClCH_2COCl$ to generate a number of products including $Cl^\bullet$, Cl^-, and CH_2CO. Unlike experiments using ClO_4^- and BF_4^- electrolytes, no high-oxidation state salts were isolated. Instead, the 1:1 and 2:1 BEDT-TTF hydrogen dichloride salts precipitate with the hydrogen dichloride anion formed in situ.

α'-(BEDT-TTF)$_2HCl_2$ (1). Crystals of **1** form as thin, square, brown plates and crystallize in the monoclinic space group $P2/c$. The brown plates are air stable for several days but gradually develop a crusty surface indicating decomposition. Figure 1 shows a packing diagram for **1** including both anions and cations and crystallographic data are presented in Tables 1 and 2.

(16) Larsen, J.; Lenoir, C. *Synthesis* **1988**, *2*, 134.
(17) Sheldrick, G. M. *SHELXTL5*; Siemens Analytical X-ray Instruments Incoporated: Madison, WI, 1995.

Table 1. Crystallographic Data for 1, 2, and 3

	1 (113 K)	**2** (233 K)	**3** (173 K)
	Crystal Data		
a, Å	7.7023(1)	12.9687(8)	12.7112(1)
b, Å	6.6140(1)	11.6077(8)	11.5778(2)
c, Å	30.1077(6)	5.6949(4)	11.3583(1)
β, deg	96.506(1)	104.688(1)	101.194(1)
V, Å^3	1523.90(4)	829.28(10)	1639.77(3)
d_{calcd}, g cm^{-3}(173 K)	1.812	1.828	1.849
empirical formula	$2[C_{10}H_8S_8]:HCl_2$	$C_{10}H_8S_8$:HCl	$C_{10}H_8S_8:HCl_2$
formula wt, g	841.20	456.55	456.55
crystal system	monoclinic	monoclinic	monoclinic
space group	*P*2/*c*	*C*2/*m*	$P2_1/c$
Z	2	2	4
F(000), electrons	854	462	924
	Structure Refinement[a]		
refinement method	full-matrix least-squares on F^2		
S, goodness-of-fit	1.082	1.049	1.155
R_1(%)/reflections	4.09/2719 > 2σ(*I*)	2.90/866 > 2σ(*I*)	3.78/2818 > 2σ(*I*)
wR_2 (%)/reflections	7.63/3483	7.78/997	9.99/2819
R_{int} (%)	7.01	2.30	2.00

[a] $R_1 = \sum(||F_o| - |F_c||)/\sum|F_o|$. $wR_2 = [\sum[w(F_o^2 - F_c^2)^2]/\sum[w(F_o^2)^2]]^{1/2}$. $S = [\sum[w(F_o^2 - F_c^2)^2]/(n-p)]^{1/2}$. $w = 1/[\sigma^2(F_o^2) + (0.0370p)^2 + 0.31p]$, $p = [\max(F_o^2,0) + 2F_c^2]/3$.

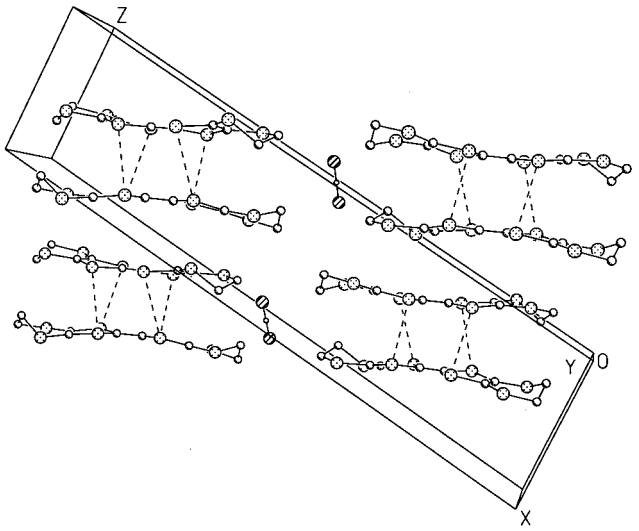

Figure 1. The packing diagram for **1** including both anions and cations. Sheets of BEDT-TTF cations are separated by layers of hydrogen dichloride anions. The hydrogen dichloride anions are symmetric and linear. The cation sheets are composed of columns of BEDT-TTF dimers. There is poor orbital overlap between cations within a column, while there is good overlap between cations in adjacent columns within the sheet.

There are two characteristic features of the α′-BEDT-TTF salts.[14] First, the BEDT-TTF cations form stacks of twisted dimers that align side-by-side to produce the donor ion sheet as illustrated in Figure 2. Second, the counterions are linear, and previously reported examples include symmetric or asymmetric triatomic ($AuBr_2^-$, $CuCl_2^-$, $IAuBr^-$) or pentaatomic ($Ag(CN)_2^-$, $Au(CN)_2^-$) anions.[12−14] Compared to other α′-BEDT-TTF salts,[12−14] **1** incorporates the shortest linear anion (6.75 Å) in the series, and consequently the unit cell volume is the smallest in the series at 1523.90(4) Å^3. The unit cell axes *a*, *b*, and *c* are all shorter in length than the other α′ materials, indicating that the "chemical compression" of the unit cell is nearly isotropic.[18] Figure 3 shows the intermolecular interactions within the BEDT-TTF network of cations. There are short S···S contacts within the twisted dimers (intrastack), but the twist, together with poor contact between dimer pairs along the stack, results in poor overlap along the *a* axis of the α′ phases.[14] Between adjacent BEDT-TTF cation stacks (interstack contacts), there are many S···S contacts less than twice the van der Waals radii sum of sulfur (3.6 Å) between inner and outer ring S atoms. The contacts, due to the parallel and coplanar arrangement of BEDT-TTF cations, lead to quasi-1D electronic and magnetic descriptions of the α′ phase.[14,19] Salt **1** has a hydrophobic environment surrounding each hydrogen dichloride anion with numerous Cl−H interactions between the anion and the ethylene hydrogen atoms on the BEDT-TTF cations. This arrangement forms a cage around each HCl_2^- ion that helps stabilize the anion. The few known examples of salts of the hydrogen dichloride anion all have a similar hydrophobic environment that has been suggested as a necessary requirement for its stabilization.[20−23]

Donor ion bond lengths are often used to assign oxidation states in charge-transfer salts of BEDT-TTF.[11,24−28] The central C═C bond of the fulvalene core of BEDT-TTF is most sensitive to changes in oxidation state, increasing in length with higher oxidation states. The central C═C bond length of 1.371(4) Å for **1** is

(18) Ward, B. H. Ph.D. Thesis, University of Florida, 1997.

(19) Parker, I. D.; Friend, R. H.; Kurmoo, M.; Day, P. *J. Phys.: Condens. Matter 1* **1989**, 5681−5688.
(20) Schroeder, L. W.; Ibers, J. A. *Inorg. Chem.* **1968**, *7*, 594−599.
(21) Kuchen, W.; Mootz, D.; Somberg, H.; Wunderlich, H.; Wussow, H. *Angew. Chem., Int. Ed. Engl.* **1978**, *17*, 869−870.
(22) Atwood, J. L.; Bott, S. G.; Coleman, A. W.; Robinson, K. D.; Whetstone, S. B.; Means, C. M. *J. Am. Chem. Soc.* **1987**, *109*, 8100−8101.
(23) Atwood, J. L.; Bott, S. G.; Means, C. M.; Coleman, A. W.; Zhang, H.; May, M. T. *Inorg. Chem.* **1990**, *29*, 467−470.
(24) Kobayashi, H.; Kato, R.; Mori, T.; Kobayashi, A.; Sasaki, Y.; Saito, G.; Enoki, T.; Inokuchi, H. *Chem. Lett.* **1984**, 179−182.
(25) Beno, M. A.; Geiser, U.; Kostka, K. L.; Wang, H. H.; Webb, K. S.; Firestone, M. A.; Carlson, K. D.; Nunez, L.; Whangbo, M.; Williams, J. M. *Inorg. Chem.* **1987**, *26*, 1912−1917.
(26) Mori, T.; Inokuchi, H. *Bull. Chem. Soc. Jpn.* **1988**, *61*, 591−593.
(27) Umland, T. C.; Allie, S.; Kuhlmann, T.; Coppens, P. *J. Phys. Chem.* **1988**, *92*, 6456−6460.
(28) Day, P.; Kurmoo, M.; Mallah, T.; Marsden, I. R.; Friend, R. H.; Pratt, F. L.; Hayes, W.; Chasseau, D.; Gaultier, J.; Bravic, G.; Ducasse, L. *J. Am. Chem. Soc.* **1992**, *114*, 10722−10729.

Table 2. Atomic Coordinates ($\times 10^4$) and Equivalent Isotropic Displacement Parameters ($Å^2 \times 10^3$) for the Three BEDT-TTF Salts[a]

α′-(BEDT-TTF)$_2$HCl$_2$ (**1**)	*x*	*y*	*z*	U_{eq}
Cl	1076(1)	−3090(1)	9883(1)	28(1)
S3	1958(1)	−1509(1)	7119(1)	18(1)
S4	3743(1)	−2849(1)	8099(1)	20(1)
S9	4378(1)	1407(1)	8335(1)	18(1)
S10	2354(1)	2767(1)	7378(1)	18(1)
S11	−166(1)	−739(1)	6256(1)	18(1)
S12	4804(1)	−4455(1)	9001(1)	25(1)
S17	99(1)	4288(1)	6579(1)	21(1)
S18	5660(1)	632(1)	9285(1)	20(1)
C1	2671(4)	252(5)	7532(1)	17(1)
C2	3476(4)	−330(5)	7941(1)	17(1)
C5	866(4)	274(4)	6753(1)	14(1)
C6	4513(4)	−2324(5)	8659(1)	16(1)
C7	1011(4)	2223(5)	6882(1)	16(1)
C8	4813(4)	−366(5)	8767(1)	16(1)
C13	−673(4)	1466(5)	5901(1)	22(1)
C14	5525(7)	−3385(6)	9544(1)	22(1)
C14′	6571(10)	−3478(15)	9390(3)	19(3)
C15	377(4)	3365(5)	6026(1)	20(1)
C16	6733(6)	−1589(6)	9538(2)	23(1)
C16′	5968(22)	−1630(12)	9624(3)	23(4)

ϵ-BEDT-TTF(HCl_2) (**2**)	*x*	*y*	*z*	U_{eq}
S1	812(1)	3743(1)	2653(1)	30(1)
S2	2203(1)	3500(1)	7602(1)	39(1)
C1	348(2)	5000	1149(4)	25(1)
C2	1551(1)	4414(2)	5275(3)	27(1)
C3	3061(4)	4490(4)	9783(8)	45(1)
C3′	3348(3)	4389(4)	8781(9)	42(1)
Cl	4806(2)	3691(1)	5146(7)	54(1)

ϵ′-(BEDT-TTF)HCl_2 (**3**)	*x*	*y*	*z*	U_{eq}
Cl1	7242(1)	3800(1)	3587(1)	38(1)
Cl2	7792(1)	1199(1)	3955(1)	41(1)
H1	7643(35)	2440(29)	3684(38)	79(16)
S3	6696(1)	6242(1)	2142(1)	20(1)
S4	8348(1)	6307(1)	331(1)	22(1)
S9	6668(1)	8764(1)	2196(1)	23(1)
S10	8276(1)	8827(1)	321(1)	21(1)
S11	5266(1)	5959(1)	3906(1)	27(1)
S12	9703(1)	6088(1)	−1473(1)	26(1)
S17	5303(1)	8971(1)	3992(1)	27(1)
S18	9671(1)	9091(1)	−1477(1)	26(1)
C1	7141(2)	7522(2)	1653(3)	17(1)
C2	7842(2)	7551(2)	853(3)	19(1)
C5	5947(2)	6883(2)	3096(2)	20(1)
C6	9054(2)	7003(2)	−629(2)	19(1)
C7	5930(2)	8055(2)	3124(2)	20(1)
C8	9021(2)	8178(2)	−629(2)	19(1)
C13	4126(2)	6896(3)	3952(3)	33(1)
C14	10568(3)	7057(3)	−2126(3)	35(1)
C15	4427(3)	7995(3)	4626(3)	38(1)
C16	10833(2)	8197(3)	−1495(3)	33(1)

[a] U_{eq} is defined as one-third of the trace of the orthogonalized U_{ij} tensor.

consistent with a donor oxidation state of $+^1/_2$ and the 2:1 stoichiometry observed with the HCl_2^- counterion.

The room temperature conductivities of the α′-(BEDT-TTF)$_2$X salts where X = $AuBr_2^-$, $Ag(CN)_2^-$, $CuCl_2^-$, and $IAuBr^-$ are ∼0.1, ∼0.03, ∼0.04, and 1.5×10^{-4} Ω^{-1} cm^{-1}, respectively.[13,19] The transport properties and the magnetic properties of the α′ materials are indicative of semiconducting behavior. The room temperature four-probe conductivity measurement on a single crystal of **1** shows that the hydrogen dichloride salt is also semiconducting with a value of $6 \pm 2 \times 10^{-4}$ Ω^{-1} cm^{-1}.

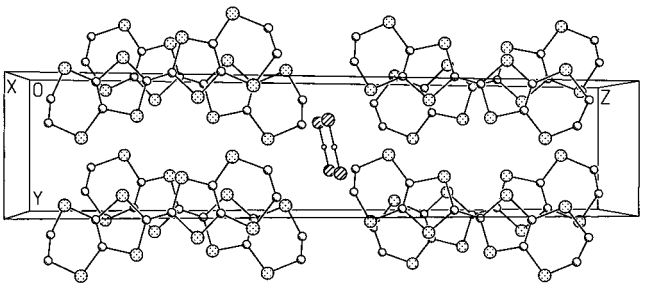

Figure 2. A view of **1** down the *a* axis showing that the BEDT-TTF dimers are not in registry, but are twisted about the central fulvalene C═C bond. This type of dimer arrangement is characteristic of α′-(BEDT-TTF)$_2$X salts.

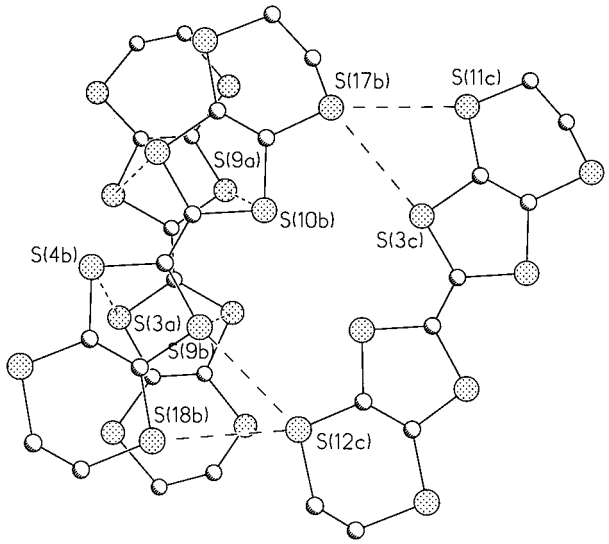

Figure 3. A view of three BEDT-TTF ions in **1** looking nearly down the stacking axis showing the intra- and intermolecular S···S close contacts. The intradimer distances are 3.560 Å for S(3a)−S(4b) and 3.601 Å for S(9a)−S(10b). The interdimer contact distances are 3.388 Å for S(9b)−S(12c), 3.429 Å for S(17b)−S(11c), 3.450 Å for S(17b)−S(3c), and 3.406 Å for S(18b)−S(12c).

The temperature dependence of the molar susceptibility, $\chi(T)$, for **1** is plotted in Figure 4. The data have been corrected for a diamagnetic core contribution, calculated using Pascal's constants,[29] of 433×10^{-6} emu/mol for α′-(BEDT-TTF)$_2$(HCl_2). The room temperature value for the corrected susceptibility is 1.1 (±0.1) $\times 10^{-3}$ emu/mol for **1**, which is slightly smaller than the "spin-only" value of 1.25×10^{-3} emu/mol for an $S = {}^1/_2$ spin system. The lower χ(300 K) value is evidence of antiferromagnetic exchange between (BEDT-TTF)$_2$ dimers. Three temperature regimes are apparent in the static susceptibility data plotted in Figure 4. The susceptibility increases gradually as the temperature is lowered from room temperature down to 125 K (region 1) where there is a slight jump in $\chi(T)$. Between 125 and 30 K (region 2), $\chi(T)$ goes through a broad maximum centered near 65 K. At the lowest temperatures (T < 20 K), the data are dominated by a Curie-like impurity (region 3). The three regions present in the susceptibility data for **1** correlate with the EPR line width (ΔH_{p-p}) data plotted in Figure 5. The EPR data were measured from 4 to 298 K on a sample of aligned crystals with the static

(29) Carlin, R. L. *Magnetochemistry*, 1st ed.; Springer-Verlag: Berlin, 1986.

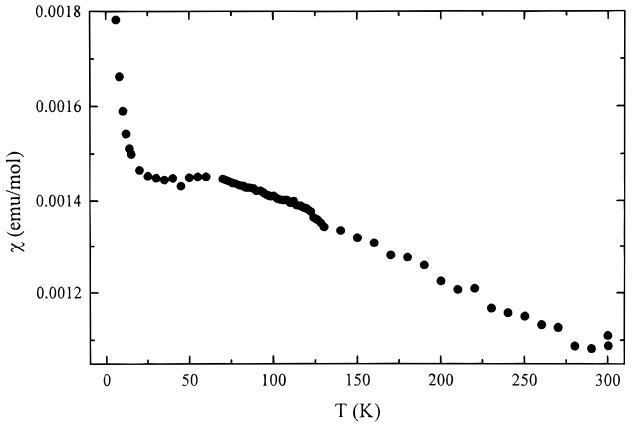

Figure 4. The magnetic susceptibility $\chi(T)$, measured in a magnetic field of 1 kG, for 31.25 mg of randomly oriented crystals of **1**. The $\chi(T)$ results show paramagnetic behavior at high temperatures with a broad maximum near 65 K, characteristic of short-range antiferromagnetic coupling in low-dimensional systems, and a strong upturn for $T < 30$ K due to paramagnetic impurities from decomposition of the hydrogen dichloride anions. An anomaly near 125 K is discussed in the text.

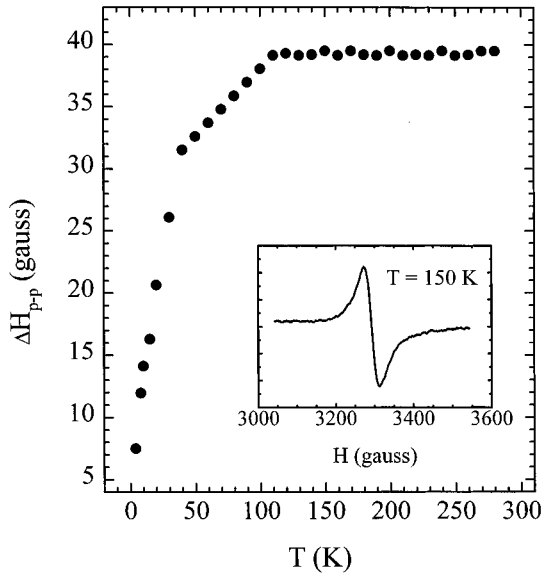

Figure 5. The EPR line width, ΔH_{p-p}, for an aligned mosaic of crystals of **1** with the static magnetic field perpendicular to the crystal faces. A representative EPR spectrum at 150 K is shown in the inset. The ΔH_{p-p} data have three characteristic regions described in the text. Region 1 has a constant line width of 39 G, while the line width gradually decreases in region 2, and sharply decreases below 40 K to a minimum of 7 G at 4 K in region 3.

magnetic field approximately perpendicular to the crystallographic *a* axis. The line width is independent of temperature in region 1 with a value of 39 G. As the temperature is lowered through region 2, the line width gradually decreases to 31 G at 40 K, followed by a rapid decrease in region 3 to 7 G at 4 K.

To investigate the origin of the 125 K anomaly seen in the magnetic data, the X-ray structure was redetermined at 113 K. The low-temperature X-ray structure reveals no major changes relative to the structure determined at 173 K. In particular, the BEDT-TTF terminal ethylene groups are still disordered at 113 K. All of the crystallographic axes undergo a slight compression by a few tenths of an angstrom which shorten the S···S contacts between BEDT-TTF cations. However, we cannot say if the slight compression is associated with the magnetic anomaly at 125 K.

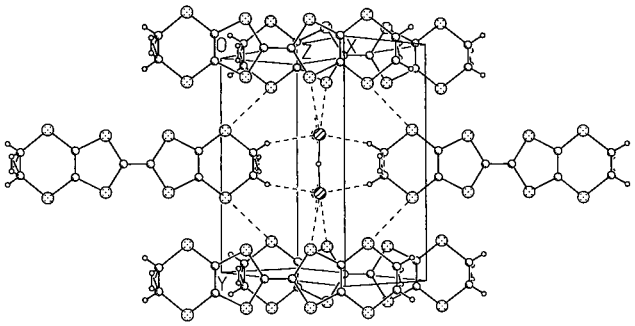

Figure 6. The crystal structure of ϵ-(BEDT-TTF)HCl_2, **2**, determined at 233 K. The BEDT-TTF monocations pack in a bond-over-ring arrangement. Each HCl_2^- anion is surrounded by a hydrophobic pocket formed from ethylene hydrogen atoms and sulfur atoms of the BEDT-TTF molecules. The CH_2 units of the cations are disordered about the mirror plane and the HCl_2^- anions are disordered about a center of inversion.

The previously studied members of the α′-(BEDT-TTF)$_2$X family have all been described as localized Mott−Hubbard systems with antiferromagnetic exchange between (BEDT-TTF)$_2$ dimers.[14] Compound **1** behaves similarly. The room temperature EPR line width of 39 G is consistent with the other α′-phase salts.[14,30] The gradual increase in $\chi(T)_{SQUID}$ to a broad maximum as the temperature is lowered is a characteristic of antiferromagnetic interactions in a low-dimensional lattice and is also seen in other α′ salts.[14] Although the general features are present, the susceptibility data are not easily fit to the commonly employed models for ideal 1D chains or 2D quadratic layer antiferromagnets. The data are complicated by the transition at 125 K, the thermal compression of the lattice at low temperature, and the considerable impurity contribution that arises from the unstable HCl_2^- anion. Nevertheless, the conductivity and magnetic data are similar to the other α′-(BEDT-TTF)$_2$X salts.

ϵ-BEDT-TTF(HCl_2) (2) and ϵ′-BEDT-TTF(HCl_2) (3). Crystals of **2** form as shiny, black, four-sided needles that are air-sensitive and degrade within minutes of exposure to air. Crystallographic data taken at 233 K for **2**, which crystallizes in the monoclinic space group *C*2/*m*, are presented in Tables 1 and 2. Figure 6 shows a packing diagram for **2** including both anions and cations. At 233 K, all BEDT-TTF monocations are equivalent, and the unit cell consists of two BEDT-TTF cations and two hydrogen dichloride anions, all located on 2/*m* sites. The terminal ethylene groups and the hydrogen dichloride anions are disordered. The salt is isostructural with the previously described salts ϵ-(BEDT-TTF)ClO_4,[15] ϵ-(BEDT-TTF)PF_6,[31] and ϵ-(BEDSe-TSeF)-PF_6.[32] As for α′-(BEDT-TTF)$_2$(HCl_2), the BEDT-TTF central C=C bond distance can be used to confirm the oxidation state of the BEDT-TTF cations in **2**. The central C=C bond distance is 1.388(4) Å, which is

(30) Kurmoo, M.; Talham, D. R.; Day, P.; Howard, J. A. K.; Stringer, A. M.; Obertelli, D. S.; Friend, R. H. *Synth. Met.* **1988**, *22*, 415−418.
(31) Bu, X.; Cisarova, I.; Coppens, P. *Acta Crystallogr.* **1992**, *C48*, 1562−1563.
(32) Kato, R.; Kobayashi, H.; Kobayashi, A.; Sasaki, Y. *Chem. Lett.* **1985**, 1943−1946.

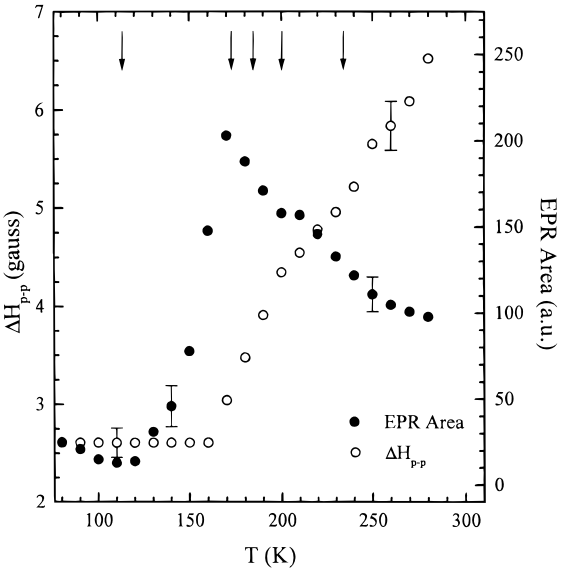

Figure 7. The EPR integrated area (filled circles) and the line width, ΔH_{p-p} (open circles), data for a single needle-like crystal of **2**. The anomaly seen near 200 K in both the integrated area and line width is associated with the anion ordering transition. The magnetic phase transition is seen near 170 K. At the lowest temperatures (down to 4 K, not shown) the data are dominated by a Curie-like impurity with constant line width. The arrows indicate temperatures at which crystallographic data were obtained.

consistent with a donor oxidation state of +1 in tetrathiafulvalene-based molecules. The hydrogen dichloride anion is unstable, as apparent from the highly air-sensitive nature of the needles. Upon contact with air, the needles quickly form a brown crust on the exterior. Reduced pressure conditions also lead to decomposition.

EPR data were obtained for a single crystal of salt **2**. Figure 7 illustrates the integrated EPR signal area and line width, ΔH_{p-p}, for **2** that were measured between 4 and 298 K with the static magnetic field approximately perpendicular to the crystallographic *c* axis. The integrated area, which is proportional to the spin magnetic susceptibility, rises gradually with decreasing temperature from 298 to 200 K, where a small kink appears. The integrated area continues to rise as the temperature is lowered to 170 K, below which point it drops sharply to a minimum at 120 K. The integrated area remains constant to about 90 K, where, at lower temperatures, an increase in the area gives evidence of a Curie-like impurity. The Curie-like behavior presumably results from decomposition of the hydrogen dichloride anion. The EPR line width as a function of temperature shows a gradual decrease as the temperature is lowered from 298 K, followed by a sharper decrease at 200 K until a minimum is reached at 160 K. At temperatures below 160 K the line width remains constant down to 4 K. Examination of the EPR integrated area and line width data shows evidence of two phase transitions, one near 200 K which has a minor effect on the magnetic structure and a magnetic phase transition between 160 and 170 K.

To investigate the nature of these transitions, a second crystal structure was solved at 173 K, and the unit cell was monitored at 113, 185, and 200 K. The 173 K structure reveals a new phase for which the crystallographic data are included in Tables 1 and 2.

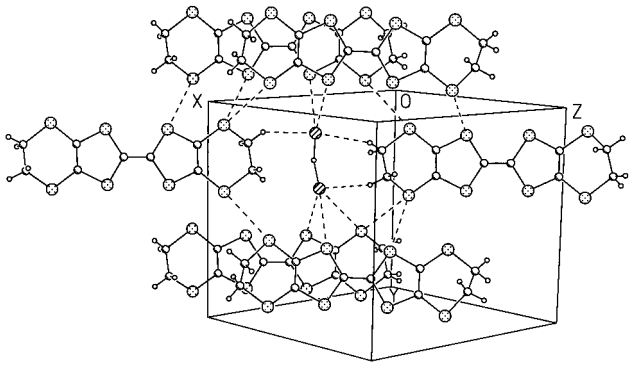

Figure 8. The crystal structure of ϵ'-(BEDT-TTF)HCl_2, **3**, determined at 173 K. Salt 3 crystallizes in the monoclinic $P2_1/c$ space group. The terminal ethylene groups of the BEDT-TTF cations and the HCl_2^- anions are ordered. Several close intra- and intermolecular S···S contacts exist between outer ring and inner ring sulfur atoms on adjacent BEDT-TTF cations, and each HCl_2^- anion sits in a hydrophobic pocket. The HCl_2^- ion is bent.

Structure **3** belongs to the $P2_1/c$ space group in contrast to the high-temperature phase, **2**, which crystallizes in $C2/m$. The cell dimensions are nearly equal for the two structures except for a doubling of the *c* axis in **3**. The structure still contains columns of HCl_2^- anions and slipped stacks of BEDT-TTF cations in a bond-over-ring arrangement (Figure 8).

The major change from **2** to **3** is ordering of the HCl_2^- ions and the terminal ethylene groups. The HCl_2^- ions now alternate between two orientations giving rise to the doubling of the unit cell. The HCl_2^- anion is bent with an Cl−H−Cl angle of 164(4)°. There are several short Cl···S and Cl···H contacts between hydrogen dichloride anions and BEDT-TTF cations. The BEDT-TTF ion network is nearly the same as in **2**, although a slight displacement of the donor ions leads to additional intermolecular close contacts. In structure **2**, one type of S···S interaction exists that involves outer ring sulfur atoms on adjacent BEDT-TTF cations. In structure **3**, two types of interactions exist, one between outer ring sulfurs and another between inner and outer ring sulfurs on adjacent BEDT-TTF cations. Because of the similarity between the two phases, we refer to the low-temperature phase as ϵ'-BEDT-TTF(HCl_2).

A unit cell determination shows the ϵ-phase exists at 200 K while the ϵ'-phase is present at 185 K. These results indicate the inflections seen in the EPR area and line width data near 200 K are related to the anion ordering structural phase transition. The anion ordering has only a minor effect on the magnetic interactions. On the other hand, the magnetic phase transition seen near 170 K in the EPR does not involve a structural change. A unit cell determination at 113 K reveals the ϵ'-phase, **3**, indicating that the same phase is present at 113, 173, and 185 K. The nature of the 170 K magnetic phase transition remains unclear. Magnetic ordering or a solid-state disproportionation reaction are possibilities that could lead to the loss of paramagnetism seen below 170 K. Unfortunately, the extreme air sensitivity of the salt has thus far precluded more detailed investigations of the physical properties.

Description of the HCl_2 Anion. Salts of the hydrogen dichloride ion are unusual but precedented.[20−23] The relatively few HCl_2^- salts known are listed in Table

Table 3. Bond Lengths and Angles for the HCl_2^- Anion in Ionic Solids

compound	H−Cl(1) (Å)	H−Cl(2) (Å)	Cl−H−Cl angle (deg)
[K·18-crown−6]HCl[a]	1.56	1.56	180
[Mg·18-crown−6]$(HCl_2)_2$[a]	1.30	2.03	161
[H_3O·18-crown−6]HCl_2[b]	1.47	1.65	168
[$PCl_2CH_3C_6H_5OCH_3$] HCl_2[c]	1.45	1.78	168
CsCl·1/3H_3OHCl_2[d]	1.57	1.57	180
α′-(BEDT-TTF)$_2HCl_2$ (**1**)[e]	1.57	1.57	180
ϵ′-(BEDT-TTF)HCl_2 (**3**)[e]	1.65(4)	1.47(3)	164(4)

[a] Reference 23. [b] Reference 22. [c] Reference 21. [d] Reference 20. [e] This work.

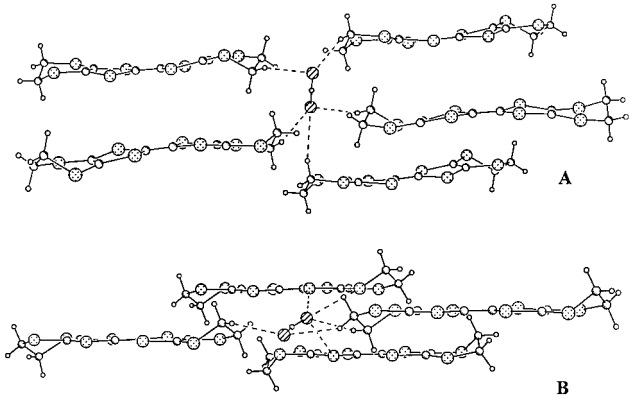

Figure 9. Views of salts **1** (A) and **3** (B) highlighting the geometry and the environment of the hydrogen dichloride anion. In salt **1**, the HCl_2^- anion is linear with equal Cl−H bond distances of 1.57 Å and a Cl−H−Cl bond angle of 180°. In salt **3** the Cl−H−Cl angle is 164(4)° with bond distances Cl(1)−H = 1.65(4) Å and Cl(2)−H = 1.47(3) Å. In both salts there are numerous intermolecular contacts between the chlorine atoms of the anions and the ethylene hydrogen atoms and the sulfur atoms of the BEDT-TTF cations.

3. Hydrogen dichloride salts all tend to lose HCl rather readily, and some are very unstable toward moisture and oxygen. Salts **1** and **2** described in this work are both air and moisture sensitive (**1** is somewhat more stable than compound **2**). Compound **1** is a shiny brown solid while **2** forms a shiny black solid, and each material maintains its integrity if kept in an inert environment. A brown crust forms if the crystals are exposed to air.

The previously isolated hydrogen dichloride salts contain molecular cations that form hydrophobic pockets for the anion. The one exception, (CsCl·$^1/_3H_3O$)HCl_2,[20] has hydronium cations as well as cesium cations stabilizing the HCl_2^- anion. The HCl_2^- environment in **1** and **3** can be seen in Figures 1 and 8, respectively, and additional perspectives are shown in Figure 9 where close contacts between the anion and donor cations are indicated. It is the terminal ethylene hydrogen atoms, as well as the sulfur atoms (low electronegativity and high polarizability), which provide the hydrophobic setting needed to stabilize the anion.

Table 3 also summarizes the H−Cl bond lengths and Cl−H−Cl bond angles of the known HCl_2^- examples. The nature of the cation influences the geometry of the anion. It has been hypothesized that strong interaction between the HCl_2^- chlorine atoms and the positive counterions results in asymmetry in the HCl_2^- anion.[22,23] In these cases, the H−Cl(1) and H−Cl(2) bond distances are not equal, and the Cl−H−Cl bond angle is less than 180°.[22,23] In compound **1** the hydrogen dichloride anions are symmetric and linear (H−Cl(1), H−Cl(2): 1.57 Å; Cl−H−Cl: 180°), whereas in salt **3** the distances are not equal and the anion is nonlinear (H−Cl(1): 1.65(4) Å; H−Cl(2): 1.47(3) Å; Cl−H−Cl: 164(4)°). These differences in the hydrogen dichloride anion bond distances and bond angles can be attributed to the different charges on the BEDT-TTF cations. The more highly charged +1 cation in salt **3** has a greater interaction with the anion than the $+^1/_2$ cation in salt **1**. In **1**, the anion−cation contacts are all through the terminal ethylene groups while in **3** there are several close Cl−S contacts in addition to the Cl−CH_2 contacts.

IV. Summary

In conclusion, three new cation-radical salts α′-(BEDT-TTF)$_2HCl_2$, ϵ-(BEDT-TTF)HCl_2, and ϵ′-(BEDT-TTF)HCl_2, have been characterized. The α′- and ϵ-phase materials were grown electrochemically from the same electrocrystallization cell. The ϵ′ salt is a low-*T* phase of ϵ-(BEDT-TTF)HCl_2 that results from an anion ordering transition. These three cation-radical salts are the first examples of BEDT-TTF salts isolated with the hydrogen dichloride, HCl_2^-, anion. Transport and magnetic susceptibility measurements show **1** is a localized Mott−Hubbard system, similar to the other known α′-BEDT-TTF salts. The 1:1 phase is paramagnetic at room temperature, but undergoes a magnetic phase transition below 170 K. The mode of BEDT-TTF packing in these systems helps to stabilize the anion. In each case, the hydrogen dichloride anion is surrounded by several BEDT-TTF cations. The C−H bonds of the BEDT-TTF engage in weak hydrogen-bonding interactions with the anions[9] providing a stabilizing hydrophobic environment.

Acknowledgment. This work was supported in part by the National Science Foundation, Grants DMR-9530453 (D.R.T.) and DMR-9200671 (M.W.M.). K.A.A. wishes to acknowledge the National Science Foundation and the University of Florida for funding the purchase of the X-ray equipment. Partial support (D.R.T.) from the donors of the Petroleum Research Fund, administrated by the ACS, is also acknowledged. We are grateful for discussions with Professor Gus Palenik.

Supporting Information Available: Tables of bond distances and angles, anisotropic displacement parameters, and hydrogen coordinates and isotropic displacement parameters for compounds **1**−**3** (11 pages); structure factors for compounds **1**−**3** (18 pages). Ordering information is given on any current masthead page.

CM9706863